AMERICAN SOCIETY FOR MICROBIOLOGY | Applied and Environmental Microbiology®

FOOD MICROBIOLOGY

Differentiation of Vegetative Cells into Spores: a Kinetic Model Applied to *Bacillus subtilis*

Emilie Gauvry,[a] Anne-Gabrielle Mathot,[a] Olivier Couvert,[a] Ivan Leguérinel,[a] Matthieu Jules,[b] Louis Coroller[a]

[a]Univ Brest, Laboratoire Universitaire de Biodiversité et Ecologie Microbienne, UMT ALTER'iX, Quimper, France
[b]Micalis Institute, INRA, AgroParisTech, Université Paris-Saclay, Jouy-en-Josas, France

ABSTRACT Spore-forming bacteria are natural contaminants of food raw materials, and sporulation can occur in many environments from farm to fork. In order to characterize and to predict spore formation over time, we developed a model that describes both the kinetics of growth and the differentiation of vegetative cells into spores. The model is based on a classical growth model and enables description of the kinetics of sporulation with the addition of three parameters specific to sporulation. Two parameters are related to the probability of each vegetative cell to commit to sporulation and to form a spore, and the last one is related to the time needed to form a spore once the cell is committed to sporulation. The goodness of fit of this growth-sporulation model was assessed using growth-sporulation kinetics at various temperatures in laboratory medium or in whey for *Bacillus subtilis*, *Bacillus cereus*, and *Bacillus licheniformis*. The model accurately describes the kinetics in these different conditions, with a mean error lower than 0.78 $\log_{10}$ CFU/ml for the growth and 1.08 $\log_{10}$ CFU/ml for the sporulation. The biological meaning of the parameters was validated with a derivative strain of *Bacillus subtilis* 168 which produces green fluorescent protein at the initiation of sporulation. This model provides physiological information on the spore formation and on the temporal abilities of vegetative cells to differentiate into spores and reveals the heterogeneity of spore formation during and after growth.

IMPORTANCE The growth-sporulation model describes the progressive transition from vegetative cells to spores with sporulation parameters describing the sporulation potential of each vegetative cell. Consequently, the model constitutes an interesting tool to assess the sporulation potential of a bacterial population over time with accurate parameters such as the time needed to obtain one resistant spore and the probability of sporulation. Further, this model can be used to assess these data under various environmental conditions in order to better identify the conditions favorable for sporulation regarding the time to obtain the first spore and/or the concentrations of spores which could be reached during a food process.

KEYWORDS Spore-forming bacteria, cellular heterogeneity, growth modeling, sporulation

Spore-forming bacteria are common contaminants of food, and represent a major source of food poisoning and food spoilage (1, 2). Bacterial cells in their vegetative or sporulated forms can be found in the environment and therefore can be natural contaminants of raw materials. The sporeformers display many physiological and enzymatic capacities. The spores are metabolically inactive, but they are commonly resistant to physical and chemical treatments applied in the food industry. In contrast, vegetative cells are more sensitive to stress, are physiologically active, and can produce degradative enzymes or toxins, form biofilms, and differentiate into resistant spores.

The aim for industrials is to limit or even avoid the presence of sporeformers in their

Citation Gauvry E, Mathot A-G, Couvert O, Leguérinel I, Jules M, Coroller L. 2019. Differentiation of vegetative cells into spores: a kinetic model applied to *Bacillus subtilis*. Appl Environ Microbiol 85:e00322-19. https://doi.org/10.1128/AEM.00322-19.

Editor Hideaki Nojiri, University of Tokyo

Address correspondence to Louis Coroller, louis.coroller@univ-brest.fr.

Received 7 February 2019
Accepted 10 March 2019
Accepted manuscript posted online 22 March 2019
Published 2 May 2019

final products and on food lines. To do so, curative means can be used, such as cleaning and whitening processes on raw materials or physical treatments, in order to reduce the load of sporeformers. Preventive means are also used in order to limit the bacterial growth by applying the cold chain or to limit the formation of biofilms with cleaning and disinfection steps. However, little attention has been paid to the formation of spores during food processes, on food lines, whereas sporulation has been observed in milk powder processes (3, 4). The sporulation leads to an increase of the spore yield in foods. Moreover, the sporulation conditions affect the quantity and the properties of resistance of spores to subsequent chemical or thermal treatments (5, 6). A better understanding of the favorable conditions (time and physicochemical properties) for sporulation can help target the location of sporulation in the plant environment and on food process lines in order to better prevent a high level and/or high resistance of spores.

The modeling of microbial responses (growth, growth/no-growth, germination, or inactivation) is useful for researchers in microbiology to quantify the microbial behavior and to test physiological hypotheses and for industrials to simulate the behavior of pathogenic or spoilage microorganisms in order to validate the process, formulation, or conditions of storage for food (7, 8). The prediction of a microbial response could be divided into two steps: (i) modeling the evolution of the microbial response over time with a kinetic model and (ii) modeling the effects of environmental factors on the kinetic parameters with a secondary model. For example, bacterial growth can be predicted over time and according to environmental factors (9–11), and some models exist to predict the resistance of spores to chemical and physical treatments (12–15).

Mechanistic or knowledge-based models for sporulation kinetics have been proposed to describe the decision-making process of sporulation initiation at the cellular and molecular levels in response to environmental stimuli (16–18). These models are complex because they require numerous parameters, most of which cannot be experimentally evaluated under industrially relevant conditions. Alternatively, empirical or phenomenological models of sporulation were proposed to describe the evolution of spore counts over time, as they are simpler to use than mechanistic models. However, empirical models do not take into account the fact that sporulation is a process of differentiation of vegetative cells into spores (19, 20), while growth and sporulation are well known to be interdependent physiological processes (21). As far as the sporulation is concerned, no model for predicting sporulation according to environmental factors is available in the literature yet and the kinetic models of sporulation have not attracted much attention in predictive microbiology.

The objectives of this work were to develop a kinetic model of sporulation which can be used as an efficient tool to assess the sporulation under laboratory conditions and, ultimately, under food and agro-industrial conditions. The model should meet some criteria based on the knowledge available on the sporulation process. At first, the sporulation kinetics must be deduced from the vegetative cell differentiation into spores. This implies that our model encompasses the kinetics of growth and sporulation. Moreover, the model parameters should characterize the heterogeneity of the time at which the vegetative cells commit to sporulation. The model should assess the sporulation efficiency and the time needed for the vegetative cells to complete the sporulation process. The biological meaning of the parameters linked to sporulation initiation is assessed by the model of the Gram-positive bacterium *Bacillus subtilis* in combination with a fluorescent reporter of sporulation initiation ($P_{spoIIAA}$ *gfp*).

RESULTS

Model development and experimental strategy. The growth of vegetative cells was described by a modified logistic model (equation 1) and their differentiation into spores over time with specific sporulation parameters: the probability (t_{max}, σ, and P_{max}; see below) of vegetative cells to give a mature spore (heat resistant) during the incubation and the time needed for the spore formation (t_f). Equation 1 is as follows:

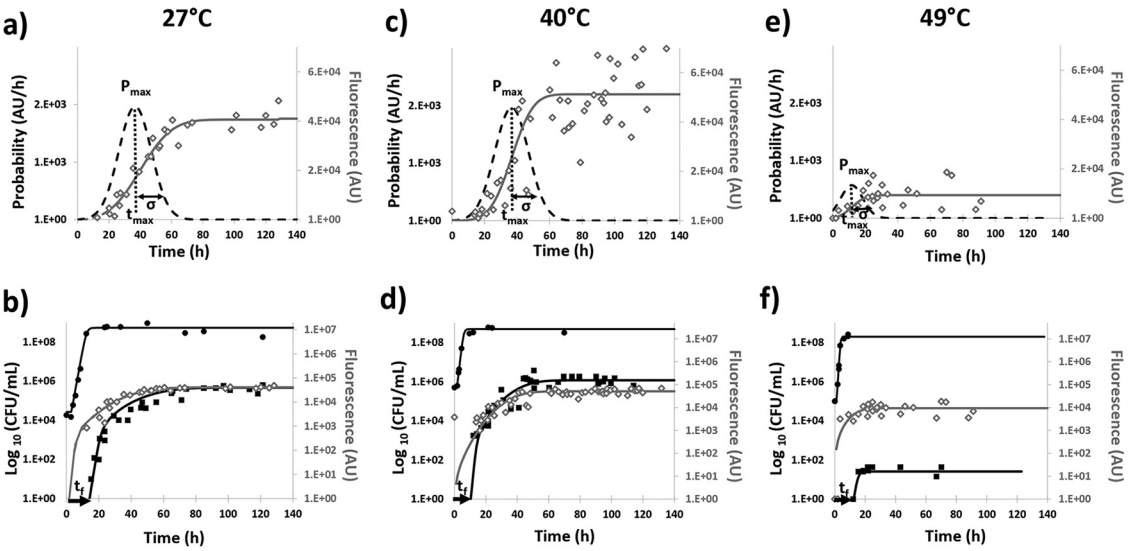

FIG 1 Fluorescence and probability kinetics (a, c, and e) and growth and sporulation kinetics (b, d, and f) of *B. subtilis* at 27°C (a and b), 40°C (c and d), and 49°C (e and f). The values of fluorescence (diamonds) were fitted with the normal density function (solid gray lines in a, c and e) and the corresponding probability densities (black dashed lines in a, c and e) with the three sporulation parameters of equation 4: P_{max}, t_{max}, and σ. The concentration of total cells (circles) and the concentration of spores (squares) over time were fitted with the growth and sporulation model in equations 1, 2, and 3 (b, d, and f). The time between the fluorescence curve ($\log_{10}$ AU on the right scale in b, d, and f) and the sporulation curve ($\log_{10}$ CFU/ml on the left scale in b, d, and f) corresponded to the time to form a spore t_f (indicated on the time scale) fitted with equation 6.

$$\ln\left[N(t_i)\right] = \begin{cases} \ln\left(N_0\right), t_i < \lambda \\ \ln\left(\dfrac{N_{\max}}{1 + \left(\dfrac{N_{\max}}{N_0}\right) \times \exp\left[-\mu_{\max} \times \left(t_i - \lambda\right)\right]}\right), t_i \geq \lambda \end{cases} \quad (1)$$

with $N(t_i)$ the bacterial concentration (CFU per milliliter) of the suspension at the time t_i, N_0 the concentration of the inoculum (CFU per milliliter), λ the lag before growth (h), μ_{max} the maximum vegetative growth rate (per hour), and N_{max} the maximal concentration of total cells (CFU per milliliter). N_{max} corresponds to the maximal concentration of vegetative cells reached at the stationary phase. Once the first spores appear, N_{max} corresponds to the total cells, i.e., the spores and the remaining vegetative cells that have not differentiated into spores.

We assumed that all vegetative cells need the same time to form a spore. The probability to sporulate was defined at the population level by the proportion of vegetative cells which initiate the sporulation over time and give a mature spore (heat resistant). At the cell level, this proportion accounts for the probability of each individual cell to sporulate over time. This probability to sporulate evolves over time following a normal distribution (equation 2), which is described with three parameters (Fig. 1a, c, and e). The first parameter is the maximal probability to sporulate (P_{max}), which accounts for the maximal proportion of vegetative cells that can sporulate in a given period of time. This parameter mainly influences the maximal concentration of spores to be produced. The second one is the time (t_{max}) at which this maximal probability to sporulate is obtained, which has an impact on the time at which the first spores appear. The third parameter is the probability scattering (σ), which has an impact on the speed of appearance of spores over time. Equation 2 is as follows:

$$P(t_i) = P_{\max} \times \left\{ \frac{1}{\sigma \times \sqrt{2\pi}} \times \exp\left[-0.5 \times \left(\frac{t_i - t_{\max}}{\sigma \times \sqrt{2}} \right)^2 \right] \right\} \quad (2)$$

with $P(t_i)$ the probability of forming a spore at time t_i (per hour) and P_{max} is the maximal proportion of vegetative cells forming spores (unitless). P_{max} was obtained at the time t_{max} (hours) at which the cell has the maximal probability of initiating sporulation and σ the standard deviation around t_{max} (hours). Let us note that the maximal probability

to sporulate at time t_{max} [$P(t_{max})$] can be calculated as follows: $P(t_{max}) = P_{max} \times \frac{1}{\sigma \times \sqrt{2\pi}}$.

The experimental strategy developed to validate the biological meaning of the sporulation parameters was based on the knowledge of the sporulation process at the physiological level. Sporulation occurs following different signals, such as nutrient starvation and communication molecules of quorum sensing, that require previous bacterial growth. After signal sensing (22), the sporulation starts with the activation (by phosphorylation) of the master regulator Spo0A to a given threshold of Spo0A~P. Once this threshold is reached, the activated master regulator activates the early sporulation genes, such as *spoIIAA*, in the predivisional cell and triggers the asymmetric division to form the mother cell and the forespore (23). The sporulation process continues according to a sequential process involving different transcription factors specific to the mother cell (σ^E and σ^K) and to the forespore (σ^F and σ^G) until the formation of a mature spore. Consequently, the strategy consisted of using a promoter fusion between the *gfp* gene and the promoter of the gene *spoIIAA* ($P_{spoIIAA}$ *gfp*) as a reporter of the initiation of sporulation. As the sporulation is mainly described for *B. subtilis* and because genetic tools are easily available for this strain, the bacterial model *B. subtilis* BSB1 was used to develop the model.

We considered that within the population, each cell of the $P_{spoIIAA}$ *gfp* strain that commits to sporulation produces the same amount of green fluorescent protein (GFP), i.e., has the same fluorescence intensity. A sporulating cell is composed of a mother cell and a forespore. The mature spore is released into the medium after lysis of the mother cell. Consequently, the fluorescence measured in a bacterial population corresponds to the fluorescence emitted by sporulating cells in addition to the fluorescence of the medium linked to the GFP molecules released in the medium following the lysis of the mother cell. The accumulation of fluorescence was directly related to the accumulation of cells that have initiated the sporulation at the time of observation and to the accumulation of spores after the time (t_f) needed to form a spore (Fig. 1b, d, and f). To simplify the model, we neglected the fluorescence that would be related to the presence of GFP molecules in the refractive spores. The fluorescence (the cell commitment to sporulation) and the concentration of sporulating cells evolved following a normal distribution function (equation 3 and Fig. 1); consequently, the probability to form a spore over time following was assessed by a normal density function (equation 3 and Fig. 1a, c, and e). Equation 3 is as follows:

$$F(t_i) = F_{max} \times \frac{1}{2} \times \left[1 + \mathrm{erf}\left(\frac{t_i - t_{max}}{\sigma \times \sqrt{2}}\right)\right] \quad (3)$$

with $F(t_i)$ the fluorescence at time t_i (arbitrary units [AU]), F_{max} the maximal fluorescence (AU), t_{max} (hours) the time at which F_{max} (AU) is obtained, σ the standard deviation around t_{max}, and erf, the error function of Gauss.

Last, the time to form a spore was assessed as time needed between cell commitment to sporulation (increase of fluorescence) and the formation of the mature spores (heat-resistant cells) (equation 4 and Fig. 1b, d, and f). Equation 4 is as follows:

$$P(t_i) = P_{max} \times N(t_i) \times \frac{1}{2} \times \left[1 + \mathrm{erf}\left(\frac{t_i - t_{max} - t_f}{\sigma \times \sqrt{2}}\right)\right] \quad (4)$$

with $N(t_i)$ the concentration of total cells (equation 1), t_{max} (hours) the time at which F_{max} (AU) was obtained, P_{max} the maximal proportion of sporulating cells, and σ (hours) the standard deviation around t_{max} (h). In this step, the values of σ and t_{max} were set to the values determined in the previous step, by fitting the fluorescence kinetics in equation 3. The two parameters fitted on the experimental sporulation kinetics were P_{max}, and the time to form a spore t_f.

Assessment of the growth and sporulation parameters of *B. subtilis* $P_{spoIIAA}$ *gfp* in modified Luria-Bertani broth at 27°C, 40°C, and 49°C. The proposed models (equations 1, 2, and 5) accurately described the growth and sporulation kinetics for *B.*

subtilis in modified Luria-Bertani broth whatever the temperature of incubation. Equation 5 is as follows:

$$S(t_i) = \begin{cases} 0, t_i < t_f \\ S(t_{i-1}) + \{[N(t_i - t_f) - S(t_{i-1})] \times P(t_i - t_f)\}, t_i > t_f \end{cases} \quad (5)$$

where $S(t_i)$ is spore concentration (CFU per milliliter) of the suspension at the time (t_i). It can be deduced from the number of spores already formed $S(t_{i-1})$ at time (t_{i-1}) and newly formed spores. These spores which are resistant at the time (t_i) are deduced from the time (t_f) needed from the commitment in sporulation to the completion of the spore (heat-resistant spores), the probability of the vegetative cells $P(t_i - t_f)$ to commit to sporulation at time $(t_i - t_f)$, and the concentration of vegetative cells which have not already committed to sporulation. This concentration of vegetative cells corresponds to the difference between the total cells $N(t_i - t_f)$ at time $(t_i - t_f)$ and the cells that are already differentiated into spore or committed in sporulation at the time $(t_i - t_f)$. These two subpopulations correspond to the all formed spores at (t_i).

The qualities of fit for growth and sporulation models reached a global root mean square error (RMSE) of 0.77 ln CFU/ml for all tested conditions (Fig. 1). The growth kinetics were slightly better fitted, with an RMSE at 0.30 ln CFU/ml, whereas the RMSE linked to the sporulation kinetics was 0.90 ln CFU/ml with a median value at 0.60 ln CFU/ml. This loss of quality of fit is due to outliers in the spore concentration and an estimation which is more uncertain. The growth and sporulation kinetics were not significantly different between the wild-type BSB1 strain and the $P_{spoIIAA}$ *gfp* strain for the three temperatures tested (likelihood ratio test, $\alpha < 5\%$). This allowed the wild-type strain to be used as a background to compute the fluorescence related to the production of GFP by the $P_{spoIIAA}$ *gfp* strain.

At 27°C, the growth rate was reduced by 35% compared to growth rate at 40°C, and the lag time was 2-fold longer, with λ values of 3.1 h and 1.6 h at 27°C and 40°C respectively. However, the kinetics of spore appearance at 27°C and 40°C were not significantly different (Table 1).

The most striking differences of growth and sporulation were observed between 27°C and 49°C. At 49°C, the growth was faster than at 27°C, with a rate almost 3 times higher and a lag before growth almost 3 times lower (Table 1). However, the sporulation was strongly inhibited at 49°C compared to that at 27°C (Fig. 1b and f). At 27°C, the fluorescence evolved gradually, from 0 h to 70 h, following a normal distribution function with a standard deviation σ of 15.9 h. The time at which the fluorescence increased the most rapidly, i.e., when the maximal probability to sporulate (P_{max}) was obtained, was at 40 h of culture. At 49°C, the fluorescence evolved faster, with a lower standard deviation (6.8 h), and the maximal probability to sporulate was obtained 25.1 h sooner (Fig. 1a and e). This less scattered probability of commitment to sporulation led to a more abrupt appearance of spores over time at 49°C than at 27°C (Fig. 1b and f). Moreover, the fast appearance of spores at 49°C was increased by a short time needed to form a heat-resistant spore (t_f) (Fig. 1b and f and Table 1).

However, fewer vegetative cells committed to sporulation at 49°C, as the maximal fluorescence reached 9.79×10^3 AU, compared to 4.11×10^4 AU at 27°C. This led to a lower concentration of spores at 49°C than at 27°C (Fig. 1b and f). Indeed, the maximal concentration of spores was 10,000 times lower. This decrease of the efficiency of sporulation could be related to the combined evolution of the three parameters (t_{max}, σ, and P_{max}) which define the probability to sporulate. The maximal probability (P_{max}) to sporulate was almost 1,000 times lower at 49°C than at 27°C. In addition, because the probability scattering (σ) was lower at 49°C, cells were able to commit to sporulation in a shorter time frame, leading to fewer cells that were able to sporulate (Fig. 1a and e and Table 1).

Application of the growth-sporulation model in whey medium and for other bacterial species. The growth and sporulation model (equations 1, 2, and 5) was used to fit the kinetics of *B. subtilis* BSB1 cultivated in whey and of *Bacillus licheniformis*

TABLE 1 Estimations of the fluorescence, the growth, and the sporulation parameters of *B. subtilis* at 27°C, 40°C, and 49°C

Data type and parameter	Meaning	Estimate (95% confidence interval)		
		27°C	40°C	49°C
Total count				
N_0 [ln (CFU/ml)]	Initial concentration of vegetative cells: inoculum size	10.2 (9.6–10.7)	13.1 (12.4–13.8)	11.5 (11.1–11.9)
λ (h)	Lag time before growth	3.1 (2.2–3.9)	1.6 (1.1–2.1)	1.2 (0.9–1.4)
μ_{max} (h^{-1})	Maximal growth rate	1.05 (0.88–1.22)	1.61 (1.33–1.88)	2.90 (2.48–3.32)
N_{max} [ln (CFU/ml)]	Maximal concentration of total cells	20.1 (19.7–20.4)	20.0 (19.8–20.2)	19.1 (18.8–19.4)
Green fluorescence				
F_{max} (AU)	Maximal fluorescence of the bacterial suspension (485/535 nm)	4.11×10^4 (3.85×10^4 to 4.35×10^4)	5.13×10^4 (4.79×10^4 to 5.47×10^4)	9.79×10^3 (7.39×10^3 to 1.22×10^4)
Heat-resistant cells (spores)				
t_{max} (h)	Time at which the maximal probability to commit to sporulation is reached	15.9 (12.5–19.4)	10.4 (5.1–15.7)	6.8 (3.3–17.0)
σ (h)	Standard deviation around t_{max}	40.0 (37.2–42.8)	36.7 (33.1–40.3)	11.6 (3.0–20.2)
P_{max}	Maximal proportion of sporulating vegetative cells	8.86×10^{-4} (4.30×10^{-4} to 1.43×10^{-3})	2.42×10^{-3} (9.14×10^{-4} to 3.03×10^{-3})	4.25×10^{-7} (1.01×10^{-7} to 7.51×10^{-7})
$P(t_{max})$ (h^{-1})	Maximal probability to sporulate	2.22×10^{-5}	5.44×10^{-5}	2.49×10^{-8}
t_f (h)	Time to form a spore from commitment to the formation of a heat-resistant spore	7.4 (7.4–7.4)	7.0 (7.0–7.0)	4.1 (4.0–4.3)

Ad978 cultivated in batch in Hageman medium supplemented with 1% brain heart infusion (BHI) at two temperatures. Kinetics from the literature (24) were used also to fit the model, like the kinetics obtained with *Bacillus cereus* AH187 cultivated in the chemically defined MODS medium (50) in aerobiosis at 37°C (Fig. 2). Because of a lack of quantitative information on the time to complete the sporulation process according to the environmental conditions and according to the species, the time to form a spore (t_f) was set to a constant value of 7 h in all cases. Let us note that such a hypothesis had an impact on the estimates of the time (t_{max}) at which the maximal probability to sporulate was reached.

The model described well the kinetics of growth and sporulation, with an error which was the same for both parts of the model (growth and sporulation) and whatever the strain or the medium was. For *Bacillus subtilis* in whey, the root mean square errors were 0.59 for growth and 0.86 for sporulation. The higher value for the sporulation part is explained by a higher variability in the observation and some outliers; i.e., the median value of error was 0.46. For *Bacillus licheniformis* in Hageman medium, the root mean square errors were 1.07 for the growth kinetics and 1.72 for the sporulation kinetics, with a median value at 1.12. Last, for *Bacillus cereus* in MODS medium, the root mean square errors were 0.29 for the growth part and 0.18 for the sporulation part.

The growth-sporulation model enabled characterization of the sporulation efficiency and different physiological strategies used by the strains. Under conditions unfavorable for growth, there were fewer formed spores, the mean time of commitment to sporulation was delayed, and its heterogeneity increased. This rising heterogeneity was greater for *Bacillus subtilis* than for *Bacillus licheniformis* kinetics, leading to earlier or later appearance of spores than under the optimal condition of growth.

DISCUSSION

Theories and design of the model. The aim of this work was to develop a model that describes accurately both the growth kinetics and the sporulation kinetics. Based

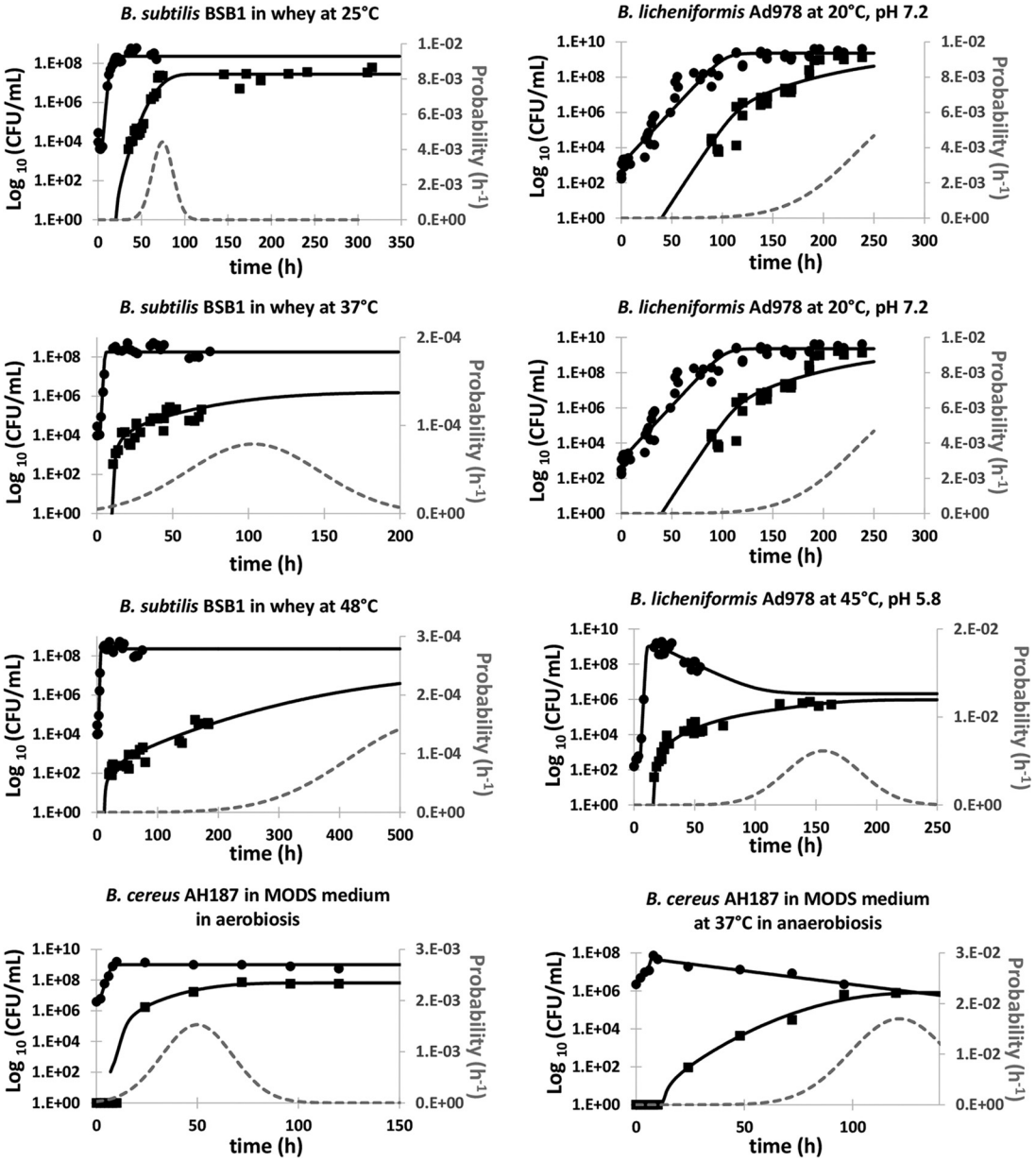

FIG 2 Growth and sporulation kinetics of three *Bacillus* species. *B. subtilis* BSB1 was grown in whey medium at 25°C, 37°C, and 48°C. *B. licheniformis* Ad978 was grown in Hageman medium supplemented with 1% BHI at 45°C and at 20°C and pH 7.2. *B. cereus* AH187 was grown in MODS medium in aerobiosis (24). The kinetics of total cells (circles) and the spores were fitted (solid lines) with the growth (equation 1) and sporulation model (equations 2 and 3). The probability to sporulate over time (equation 2) is indicated in gray dashed lines.

on a classical growth model, the sporulation kinetics was precisely described using three parameters related to the decision-making process of vegetative cells to sporulate and the time needed to complete the process.

The logistic model of growth (equation 1) is largely used to describe the bacterial growth. It describes the growth kinetics with the initial concentration of cells, the lag before growth, the growth rate and the maximal concentration of total cells. Similarly, some models were developed to describe the sporulation kinetics with parameters such as the lag before the appearance of the first spores, the sporulation rate, and the maximal concentration of spores. However, these models dissociate the growth and the sporulation, whereas these two bacterial processes are physiologically intertwined (25). This statement was supported by previous

observations on other species of *Bacillus*, as a correlation between the growth rate and the sporulation rate was found (19).

The decision-making process to sporulate was defined elsewhere at the cell level (26–28) and was translated at the population level by the probability to sporulate (*P*). The sporulation decision-making process of vegetative cells is directly linked to both the growth rate and the bacterial density (25), which evolve themselves over time following the growth kinetic. Therefore, we suggested that the probability of sporulation evolves over time also. This hypothesis is supported by recent works (29) which showed that the time of sporulation (or the time at which the cells enter into sporulation) is heterogeneous among a bacterial population. For many biological processes, heterogeneity is the result of the multiscale organization of life, as explained elsewhere (30). The heterogeneity of sporulation between cells can be explained at the molecular and cellular levels by stochastic variations (31). The heterogeneity of sporulation over time can be explained because the heterogeneity depends on nutrient starvation, which becomes increasingly severe over time, and depends on quorum sensing molecules that accumulate over time. Moreover, the sporulation heterogeneity also rises with the heterogeneity of other decision-making cell processes, such as entry into competence, cannibalism, or dormancy (32, 33), that delay the entry into sporulation. Ultimately, once the sporulation is initiated by vegetative cells, the process takes some hours to achieve until it forms a mature spore, which defines the sporulation parameter (t_f).

Quantitative and qualitative information brought by the sporulation parameters. The growth-sporulation model allowed accurate description of the growth and sporulation kinetics and allowed computation of the time to obtain the first spore in the culture, the speed of appearance of spores, and the maximal concentration of spores. Various curves shapes of growth and sporulation kinetics (fast and low kinetics) obtained for three *Bacillus* species and under different environmental conditions were accurately described with the model (Fig. 1 and 2). The model was even more accurate than sporulation models previously suggested in the literature (19, 20) with lower RMSE values. In particular, these early models did not succeed in describing the smooth emergence of spores as observed at 40°C and 27°C. In some cases, the use of these early models led to aberrant estimations of the time needed to see the first spores and the maximal concentration of spores.

The study of the sporulation parameters gives information on the sporulation behavior of vegetative cells over time at the physiological level. The probability to sporulate over time is described with a normal density function involving three parameters. The maximal probability (P_{max}) to sporulate accounts for the sporulation efficiency and explains why the sporulation yield is much higher at 40°C and 27°C than at 49°C. The low proportions of cells which sporulated at 49°C may be the result of the rapid physicochemical degradation of the medium provoked by such a high temperature. A simple hypothesis is that the deterioration of the growth medium may alter the cell decision-making and consequently advantage or disadvantage certain physiological processes. For *B. subtilis* cultivated in Luria-Bertani broth at 49°C, this hypothesis is supported by the rapid cell decline observed at 49°C after the maximal concentration of spores was reached (Fig. 2).

The probability scattering (σ) assesses how synchronous the bacterial population is for initiating sporulation. For *B. subtilis*, the sporulation was more synchronous at 40°C than at 49°C in laboratory medium (see σ values in Table 1). Similarly, the species *B. licheniformis*, genetically close to *Bacillus subtilis*, displays the same characteristics, as the sporulation is less synchronous at 45°C than at 20°C (see Table 2 and Fig. 2). At least two hypotheses can explain this observation. First, the temperature affects the membrane fluidity by modifying its composition in fatty acids, which, in turn, is known to affect the activity of the sensors such as the histidine kinase KinA (34). Second, differentiation processes such as the entry into competence or the cannibalism are impacted by environmental factors. For instance, *B. subtilis* displays cannibalistic behavior at 40°C but not at 45°C (35). Consequently, we can reasonably assume that there

TABLE 2 Estimations of the growth, death, and sporulation parameters of three *Bacillus* species grown under different conditions of culture

Data type and parameter	Meaning	Estimate (95% confidence interval)					
		B. subtilis BSB1 in whey			*B. licheniformis* Ad978 in Hageman medium		*B. cereus* AH187 in MODS medium, 37°C
		25°C	37°C	48°C	45°C	20°C	
Total count							
N_0 [ln (CFU/ml)]	Initial concentration of vegetative cells	8.94 (8.35–9.53)	9.58 (8.79–10.37)	9.6 (8.9–10.3)	6.6 (5.0–7.2)	7.0 (6.4–7.6)	15.2 (13.7–16.7)
λ (h)	Lag time before growth	5.0 (4.75–5.25)	2.2 (1.5–3.0)	2.3 (1.7–2.9)	5.0 (4.1–6.0)	0.0 (−4.3–4.3)	1.5 (0.0–3.6)
μ_{max} (h^{-1})	Maximal growth rate	1.10 (0.90–1.30)	3.29 (1.90–4.67)	2.63 (1.83–3.43)	1.25 (1.11–1.40)	0.14 (0.13–0.15)	0.98 (0.47–1.49)
N_{max} [ln (CFU/ml)]	Maximal concentration of total cells	19.2 (18.9–19.6)	19.0 (18.7–19.3)	19.2 (19.0–19.5)	21.2 (20.9–21.6)	21.6 (21.2–21.9)	20.7 (20.1–21.4)
Heat-resistant cells (spores)							
t_{max} (h)	Time at which the maximal probability to commit to sporulation is reached	12.0 (10.2–13.9)	43.8 (30.7–56.8)	132.8 (86.8–178.7)	20.7 (17.9–23.5)	297.7 (263.8–331.5)	50.0 (16.2–83.7)
σ (h)	Standard deviation around t_{max}	74.4 (67.7–81.1)	103.2 (77.5–128.9)	548.7 (253.2–844.1)	4.0 (2.9–5.2)	65.2 (55.3–75.0)	17.6 (0.0–37.0)
P_{max}	Maximal proportion of sporulating vegetative cells	0.13 (0.05–0.22)	0.01 (0.00–0.02)	0.05 (0.00–0.23)	1.00 (0.40–1.60)	1.00 (0.29–1.71)	0.07 (0.0–0.15)

are fewer differentiation opportunities at 49°C than at 40°C, which leads to a lower sporulating population heterogeneity at 49°C.

Associated with σ value, the time (t_{max}) at which P_{max} is obtained allows assessment of the time at which the first cells initiate the sporulation. It could be assessed by the product of the probability to sporulate with the number of total cells for a given volume of suspension. The time needed to observe the first spores be could be estimated for various size of volumes of analyte (1 to 10 ml) or various sizes of batches.

Last, the time to form a spore (t_f) brings information on the time needed to complete the sporulation process according to environmental conditions. As growth and sporulation share enzymatic machineries (36–38), the time to form a spore is likely to be correlated with the growth rate. This could explain why the sporulation completed faster at 49°C, at which bacterial cells grew faster than at 40°C and 27°C. Nevertheless, dedicated experiments are required to address this issue.

In summary, a kinetic model was developed to describe both growth and sporulation as a process of differentiation from vegetative cells into spores. On the one hand, the model describes the growth with the classical logistic model of Kono modified by Rosso et al. (39). On the other hand, the sporulation kinetics can be described independently of the growth kinetics by two specific parameters: the time to form a spore and the probability to form a spore over time. The biological meaning of the sporulation parameters was experimentally assessed, providing both qualitative information at the physiological level on the sporulation process and quantitative information. The sporulation parameters revealed that at suboptimal sporulation temperatures (e.g., 49°C), vegetative cells commit to sporulation more synchronously, in smaller amounts and belatedly compared to the case at optimal temperature (e.g., 40°C). Data of interest such as the time necessary for the formation of the first spore or the maximal concentration of spores can be calculated. The model allows estimation of these values more accurately than previous models in the literature. The model developed in this study thus constitutes a good tool to describe and assess the effects of diverse environmental conditions on the growth and sporulation behaviors. Ultimately, these studies will allow identification of the favorable conditions for sporulation regarding either the speed of the process (assessed with the time to see the first spore) and/or the concentration of spores which could be produced (assessed with the maximal concentration of spores).

MATERIALS AND METHODS

Biological material and strain storage. The prototrophic *B. subtilis* strain BSB1, a *trp*$^+$ derivative of *B. subtilis* strain 168, was used in this work (40, 41). The BSB1 derivative strain carrying the $P_{spoIIAA}$ *gfp* transcriptional fusion was built by transformation of genomic DNA from strain AC699 (kindly provided by Arnaud Chastanet, Micalis Institute, Jouy-en-Josas, France) using natural competence. Strain AC699 is a derivative of the *B. subtilis* strain PY79 (42) containing the *gfpmut2* gene under the control of the *spoIIAA* promoter (*amyE*::$P_{spoIIAA}$ *gfp cat*), which is a marker of the early stage of sporulation and controls the initiation of sporulation. The transcription of this gene is not subject to intrinsic noise, which means that the heterogeneity of activation of this gene is not due to stochastic processes but is correlated to the sensing of the environment (43). GFP_{mut2} is stable for 7 days and in a pH range of 5.0 to 10.0 (44–46).

Regarding the transformation procedure, *B. subtilis* was grown overnight on Luria-Bertani plates (Difco, Becton, Dickinson and Company) at 37°C. After incubation, a colony was resuspended in MG1 medium composed of MG medium containing 2 g/liter of $(NH_4)_2SO_4$ (Merck, Germany), 1 g/liter of $Na_3C_6H_5O_7$ (Carlo Erba Reagents, France), 14 g/liter of $K_2HPO_4{\cdot}3H_2O$ (Sigma-Aldrich, USA), 6 g/liter of KH_2PO_4 (Sigma-Aldrich), 0.5% glucose (Merck), and 15.6 mM $MgSO_4$ (Merck), with 0.025% Casamino Acids and 0.1% yeast extract (Difco, Becton, Dickinson and Company) added, for 4 h 30 min at 37°C under agitation at 200 rpm. A 10-fold dilution was then carried out in MG2 composed of MG medium to which 0.012% Casamino Acids, 0.025% yeast extract, $MgSO_4$, and $Ca(NO_3)_2$ (8 mM; Merck) had been added. The suspension was incubated for 1 h 30 min at 37°C under agitation at 200 rpm (47). A total of 200 μl of the suspension in MG2 was added to 0.1 μl of genomic DNA extracted from strain AC699 with a High Pure PCR template extraction kit (Roche Dignostics, Meylan, France) and incubated for 30 min at 37°C. Clones were selected on Luria-Bertani broth containing 5 μg/ml of chloramphenicol after incubation for 24 h at 37°C. The inability of the $P_{spoIIAA}$ *gfp* strain to degrade starch (as the reporter fusion is inserted at the *amyE* locus) was also verified on starch plates with iodine revelation.

Regarding the storage of *B. subtilis* strains, each selected colony was isolated on Luria-Bertani plates and incubated overnight at 37°C. A colony was resuspended in Luria-Bertani broth (Difco, Becton, Dickinson and Company) under agitation at 100 rpm at 37°C for 4 h. From this preculture, a 100-fold

dilution was performed in 100 ml of Luria-Bertani broth in flasks, under the same culture conditions, for 3 h. A second dilution was then performed under the same conditions. When the early stationary phase was reached after a 5-h culture, glycerol was added to the bacterial suspension at a final concentration of 25% (wt/wt) in cryovials. The bacterial cells in cryovials were stored at −80°C.

The strain *B. licheniformis* Ad978 was kindly provided by the Agro-Industrial Technical Institute ADRIA (Quimper, France) in cryovials containing vegetative cells conserved in BHI (Biokar Diagnostics, Beauvais, France) (70%) and glycerol (30%) at −20°C at an average concentration of 1.0×10^8 CFU/ml.

Conditions of inoculation and incubation. Before each inoculation, the absence of spores in the inoculum was ensured by heating at 80°C for 10 min the original suspension and plating 1 ml on agar plates. The absence of colonies on the plates after 24 h of incubation at 37°C confirmed the absence or low level of resistant spores in the inoculum (<1 CFU/ml).

Vegetative cells of *B. subtilis* BSB1 and the $P_{spoIIAA}$ *gfp* strain were inoculated from the cryovials at an initial concentration of 1,000 CFU/ml in 250-ml flasks filled with 100 ml of Luria-Bertani broth (Biokar Diagnostics, Beauvais, France) supplemented with sporulation salts (48). Theses flasks were incubated under agitation at 100 rpm at 40°C, which is close to the optimal growth temperature, or at two temperatures suboptimal for growth and sporulation (27°C and 49°C). The incubation was performed in darkness to prevent excitation and degradation of the GFP produced by the $P_{spoIIAA}$ *gfp* strain.

Following the same procedure for inoculation, *B. subtilis* BSB1 was also incubated 250-ml flasks filled with 100 ml of whey at 25°C, 37°C, or 48°C, with an initial inoculum of 1,000 CFU/ml. The whey was prepared from dehydrated cheddar whey powder provided by ADRIA (Quimper, France) at a concentration of 65 g/liter. The solution was sterilized on filters with pores of 0.22 μm (EMD Millipore Steritop; Fisher Scientific, France).

Batch cultures of *B. licheniformis* Ad978 were performed in bioreactor (Applikon Biotechnology, Holland) in 2 liters of Hageman medium (48) supplemented with 1% BHI, under agitation at 300 rpm and aeration at 3 liters/min, under two conditions: at 45°C and pH 7.2 and at 20°C and pH 7.2. The pH was maintained at a constant by addition of chlorydric acid (0.1 M) or sodium hydroxide (0.1 M).

Monitoring the kinetics of growth, sporulation, and fluorescence. The growth kinetics were monitored by pouring 1 ml of the relevant dilution of the incubated medium (modified Luria-Bertani broth, whey, or Hageman medium) into nutrient agar (Biokar Diagnostics, Beauvais, France). Enumeration of colonies was performed after incubation of the plates for 24 h at 37°C (ISO 7218). Sporulation was monitored by enumerating cells resistant to a 10-min heat treatment at 80°C. The heat treatment was applied to 100 μl of suspension samples using 200-μl capillary tubes which are sealed before the treatment and aseptically broken after it (5).

The green fluorescence emitted by the total suspensions of the wild-type BSB1 (used as a reference for background fluorescence) and $P_{spoIIAA}$ *gfp* strains was monitored over time. A total of 100 μl of the incubated suspension obtained in shaking flasks was distributed in microplates, and measurements were performed with a microplate photometer (VICTOR X; Perkin Elmer) equipped with an excitation filter at 485 nm and emission filter at 535 nm for green fluorescence measurement. The duration of the excitation was 1.0 s.

The autofluorescence of wild-type strain BSB1 was used as the background fluorescence. The wild-type and $P_{spoIIAA}$ *gfp* BSB1 strains were concomitantly cultivated. The fluorescence emitted by wild-type BSB1 was subtracted from the fluorescence emitted by the $P_{spoIIAA}$ *gfp* strain at each time point to assess the fluorescence associated with the production of GFP, hereafter referred as the "fluorescence." The detection threshold of the microplate was around 10^3 AU/ml.

Model development. The model of growth and sporulation can be divided into two modules. The growth was fitted by the logistic model of Kono modified by Rosso et al. (39) (equation 1).

The sporulation kinetics were deduced from growth kinetics (equation 5).

The probability to commit to sporulation was defined as the proportion of cells that commit to sporulation over time. Previous works have shown that vegetative cells of a bacterial population do not initiate the sporulation at the same time (29). Consequently, the probability of sporulation evolves over time. In order to describe this evolution, the use of four density functions (the Gaussian, the Weibull, the lognormal, and the Gamma laws) was assessed by various criteria: the biological significance of the parameters of each model, the parsimonious number of parameters, and the quality of fit of the kinetics with the RMSE statistical criterion (see equation 7 below). This led us to choose the Gaussian probability density which was weighted by the maximal proportion P_{max} of the vegetative cells to sporulate (equation 2). Finally, the sporulation part of the model combines equations 2 and 5.

Experimental assessment of the growth and the sporulation parameters. The growth and the sporulation parameters of the model (equations 1, 2, and 5) were estimated in a three-step procedure with the cultures of the $P_{spoIIAA}$ *gfp* strain of *B. subtilis*. In the first step, the primary growth model was fitted to the experimental counts (ln CFU per milliliter) to estimate the growth parameters (N_0, λ, μ_{max}, and N_{max}) with equation 1. In the second step, the fluorescence kinetics were fitted with the cumulative distribution function for the normal distribution (equation 3).In the third step, the time taken to form a spore (t_f) and the maximal proportion of sporulating cells (P_{max}) were estimated. To do so, the sporulation curves were fitted with the corresponding distribution function of equation 3, with the modification in equation 4.

Statistical procedures and analysis. The growth and sporulation parameters of equations 1 to 6 were estimated by minimizing the error sum of squares (ESS; fmincon, Optimization Toolbox; MATLAB 7.9.0; The Math-works, Natick, USA) (equation 6). Ninety-five percent confidence intervals were estimated with the nlparci function of the Optimization Toolbox (MATLAB 7.9.0; The Math-works, Natick, USA). Equation 6 is as follows:

$$\mathrm{ESS} = \Sigma \left(y_i - \hat{y}_i\right)^2 \quad (6)$$

with y_i the experimental data for the concentration of total cells or spores (log CFU per milliliter) or fluorescence (AU) and $\hat{y}_i$ the value calculated with the model.

The goodness of fit of the model was assessed with the root mean square error (RMSE), determined by equation 7:

$$\mathrm{RMSE} = \sqrt{\frac{\mathrm{ESS}}{n-p}} \quad (7)$$

with ESS the error sum of squares calculated in equation 6, *n* the number of experimental data, and *p* the number of parameters of the model.

The likelihood ratio test (49) was used to check that the growth and sporulation kinetics were not significantly different between the wild-type BSB1 and $P_{spoIIAA}$ *gfp* strains. The growth and sporulation parameters were estimated for both strains. In order to compare the quality of fit with the model with fitted parameters or inputs, the likelihood ratio (S_L) was calculated by equation 8 (49):

$$S_L = n \times \ln\left(\frac{\mathrm{ESS}_{\mathrm{constrained}}}{\mathrm{ESS}_{\mathrm{unconstrained}}}\right) \quad (8)$$

where *n* is the number of experimental data, $\mathrm{ESS}_{\mathrm{unconstrained}}$ is the ESS obtained by fitting the eight growth and sporulation parameters to the kinetics of the $P_{spoIIAA}$ *gfp* strain, and $\mathrm{ESS}_{\mathrm{constrained}}$ is the ESS obtained with the same eight kinetics but using the 8 parameters estimated for strain BSB1 as inputs. The value was compared with the chi-squared value (15.51) that corresponds to a degree of freedom of 8 and a tolerance threshold α of 5%.

ACKNOWLEDGMENTS

We thank Arnaud Chastanet (Micalis, Jouy-en-Josas, France) for providing the *B. subtilis* AC699 strain.

This work was supported by Quimper Bretagne Occidentale and by a doctoral grant from the regional council of Brittany (Région Bretagne, France).

We declare no conflict of interest.

REFERENCES

1. Carlin F. 2011. Origin of bacterial spores contaminating foods. Food Microbiol 28:177–182. https://doi.org/10.1016/j.fm.2010.07.008.
2. Postollec F, Mathot A-G, Bernard M, Divanac'h M-L, Pavan S, Sohier D. 2012. Tracking spore-forming bacteria in food: from natural biodiversity to selection by processes. Int J Food Microbiol 158:1–8. https://doi.org/10.1016/j.ijfoodmicro.2012.03.004.
3. Dubnau D, Mirouze N. 2013. Chance and necessity in *Bacillus subtilis* development. Microbiol Spectr 1:TBS-0004-2012. https://doi.org/10.1128/microbiolspectrum.TBS-0004-2012.
4. Faille C, Bénézech T, Midelet-Bourdin G, Lequette Y, Clarisse M, Ronse G, Ronse A, Slomianny C. 2014. Sporulation of *Bacillus* spp. within biofilms: a potential source of contamination in food processing environments. Food Microbiol 40:64–74. https://doi.org/10.1016/j.fm.2013.12.004.
5. Baril E, Coroller L, Postollec F, Leguerinel I, Boulais C, Carlin F, Mafart P. 2011. The wet-heat resistance of *Bacillus weihenstephanensis* KBAB4 spores produced in a two-step sporulation process depends on sporulation temperature but not on previous cell history. Int J Food Microbiol 146:57–62. https://doi.org/10.1016/j.ijfoodmicro.2011.01.042.
6. Leguérinel I, Couvert O, Mafart P. 2007. Modelling the influence of the sporulation temperature upon the bacterial spore heat resistance, application to heating process calculation. Int J Food Microbiol 114:100–104. https://doi.org/10.1016/j.ijfoodmicro.2006.10.035.
7. Ross T, McMeekin TA. 2003. Modeling microbial growth within food safety risk assessments. Risk Anal 23:179–197. https://doi.org/10.1111/1539-6924.00299.
8. Membré J-M, Lambert R. 2008. Application of predictive modelling techniques in industry: From food design up to risk assessment. Int J Food Microbiol 128:10–15. https://doi.org/10.1016/j.ijfoodmicro.2008.07.006.
9. Pinon A, Zwietering M, Perrier L, Membre J-M, Leporq B, Mettler E, Thuault D, Coroller L, Stahl V, Vialette M. 2004. Development and validation of experimental protocols for use of cardinal models for prediction of microorganism growth in food products. Appl Environ Microbiol 70:1081–1087. https://doi.org/10.1128/AEM.70.2.1081-1087.2004.
10. de Souza Sant'Anna A. 2017. Quantitative microbiology in food processing: modeling the microbial ecology. John Wiley & Sons, Chichester, UK.
11. Doyle MP, Buchanan RL (ed). 2012. Food microbiology: fundamentals and frontiers, 4th ed. ASM Press, Washington, DC.
12. Nguyen Thi Minh H, Durand A, Loison P, Perrier-Cornet J-M, Gervais P. 2011. Effect of sporulation conditions on the resistance of *Bacillus subtilis* spores to heat and high pressure. Appl Microbiol Biotechnol 90:1409–1417. https://doi.org/10.1007/s00253-011-3183-9.
13. Mah J-H, Kang D-H, Tang J. 2008. Effects of minerals on sporulation and heat resistance of *Clostridium sporogenes*. Int J Food Microbiol 128:385–389. https://doi.org/10.1016/j.ijfoodmicro.2008.10.002.
14. Mtimet N, Trunet C, Mathot A-G, Venaille L, Leguérinel I, Coroller L, Couvert O. 2015. Modeling the behavior of *Geobacillus stearothermophilus* ATCC 12980 throughout its life cycle as vegetative cells or spores using growth boundaries. Food Microbiol 48:153–162. https://doi.org/10.1016/j.fm.2014.10.013.
15. Peña WEL, Massaguer PRD, Teixeira LQ. 2009. Microbial modeling of thermal resistance of *Alicyclobacillus acidoterrestris* CRA7152 spores in concentrated orange juice with nisin addition. Braz J Microbiol 40:601–611. https://doi.org/10.1590/S1517-83822009000300024.
16. De Jong H, Geiselmann J, Batt G, Hernandez C, Page M. 2004. Qualitative simulation of the initiation of sporulation in *Bacillus subtilis*. Bull Math Biol 66:261–299. https://doi.org/10.1016/j.bulm.2003.08.009.
17. Jabbari S, Heap JT, King JR. 2011. Mathematical modelling of the sporulation-initiation network in *Bacillus subtilis* revealing the dual role of the putative quorum-sensing signal molecule phrA. Bull Math Biol 73:181–211. https://doi.org/10.1007/s11538-010-9530-7.
18. Schultz D, Wolynes PG, Ben Jacob E, Onuchic JN. 2009. Deciding fate in adverse times: sporulation and competence in *Bacillus subtilis*. Proc Natl Acad Sci U S A 106:21027–21034. https://doi.org/10.1073/pnas.0912185106.
19. Baril E, Coroller L, Couvert O, El Jabri M, Leguerinel I, Postollec F, Boulais C, Carlin F, Mafart P. 2012. Sporulation boundaries and spore formation kinetics of *Bacillus* spp. as a function of temperature, pH and a(w). Food Microbiol 32:79–86. https://doi.org/10.1016/j.fm.2012.04.011.
20. Das S, Sen R. 2011. Kinetic modeling of sporulation and product formation in stationary phase by *Bacillus coagulans* RK–02 vis-à-vis other bacilli. Biore-

sour Technol 102:9659–9667. https://doi.org/10.1016/j.biortech.2011.07.067.
21. Narula J, Kuchina A, Lee DD, Fujita M, Süel GM, Igoshin OA. 2015. Chromosomal arrangement of phosphorelay genes couples sporulation and DNA replication. Cell 162:328–337. https://doi.org/10.1016/j.cell.2015.06.012.
22. Sonenshein AL. 2000. Control of sporulation initiation in *Bacillus subtilis*. Curr Opin Microbiol 3:561–566. https://doi.org/10.1016/S1369-5274(00)00141-7.
23. Molle V, Fujita M, Jensen ST, Eichenberger P, González-Pastor JE, Liu JS, Losick R. 2003. The Spo0A regulon of *Bacillus subtilis*. Mol Microbiol 50:1683–1701. https://doi.org/10.1046/j.1365-2958.2003.03818.x.
24. Abbas AA, Planchon S, Jobin M, Schmitt P. 2014. Absence of oxygen affects the capacity to sporulate and the spore properties of *Bacillus cereus*. Food Microbiol 42:122–131. https://doi.org/10.1016/j.fm.2014.03.004.
25. Narula J, Kuchina A, Zhang F, Fujita M, Süel GM, Igoshin OA. 2016. Slowdown of growth controls cellular differentiation. Mol Syst Biol 12:871. https://doi.org/10.15252/msb.20156691.
26. Higgins D, Dworkin J. 2012. Recent progress in *Bacillus subtilis* sporulation. FEMS Microbiol Rev 36:131–148. https://doi.org/10.1111/j.1574-6976.2011.00310.x.
27. Maughan H, Nicholson WL. 2004. Stochastic processes influence stationary-phase decisions in *Bacillus subtilis*. J Bacteriol 186:2212–2214. https://doi.org/10.1128/JB.186.7.2212-2214.2004.
28. Narula J, Devi SN, Fujita M, Igoshin OA. 2012. Ultrasensitivity of the *Bacillus subtilis* sporulation decision. Proc Natl Acad Sci U S A 109:E3513–E3522. https://doi.org/10.1073/pnas.1213974109.
29. Mutlu A, Trauth S, Ziesack M, Nagler K, Bergeest J-P, Rohr K, Becker N, Höfer T, Bischofs IB. 2018. Phenotypic memory in *Bacillus subtilis* links dormancy entry and exit by a spore quantity-quality tradeoff. Nat Commun 9:69. https://doi.org/10.1038/s41467-017-02477-1.
30. Komin N, Skupin A. 2017. How to address cellular heterogeneity by distribution biology. Curr Opin Syst Biol 3:154–160. https://doi.org/10.1016/j.coisb.2017.05.010.
31. Ryall B, Eydallin G, Ferenci T. 2012. Culture history and population heterogeneity as determinants of bacterial adaptation: the adaptomics of a single environmental transition. Microbiol Mol Biol Rev 76:597–625. https://doi.org/10.1128/MMBR.05028-11.
32. Süel GM, Garcia-Ojalvo J, Liberman LM, Elowitz MB. 2006. An excitable gene regulatory circuit induces transient cellular differentiation. Nature 440:545–550. https://doi.org/10.1038/nature04588.
33. Suel GM, Kulkarni RP, Dworkin J, Garcia-Ojalvo J, Elowitz MB. 2007. Tunability and noise dependence in differentiation dynamics. Science 315:1716–1719. https://doi.org/10.1126/science.1137455.
34. Strauch MA, de Mendoza D, Hoch JA. 1992. *cis*-Unsaturated fatty acids specifically inhibit a signal-transducing protein kinase required for initiation of sporulation in *Bacillus subtilis*. Mol Microbiol 6:2909–2917. https://doi.org/10.1111/j.1365-2958.1992.tb01750.x.
35. Nandy SK, Prasad V, Venkatesh KV. 2008. Effect of temperature on the cannibalistic behavior of *Bacillus subtilis*. Appl Environ Microbiol 74:7427–7430. https://doi.org/10.1128/AEM.00683-08.
36. Mendez MB, Orsaria LM, Philippe V, Pedrido ME, Grau RR. 2004. Novel roles of the master transcription factors Spo0A and σB for survival and sporulation of Bacillus subtilis at low growth temperature. J Bacteriol 186:989–1000. https://doi.org/10.1128/JB.186.4.989-1000.2004.
37. Reder A, Gerth U, Hecker M. 2012. Integration of σB activity into the decision-making process of sporulation initiation in *Bacillus subtilis*. J Bacteriol 194:1065–1074. https://doi.org/10.1128/JB.06490-11.
38. Reder A, Albrecht D, Gerth U, Hecker M. 2012. Cross-talk between the general stress response and sporulation initiation in *Bacillus subtilis*—the σ(B) promoter of spo0E represents an AND-gate. Environ Microbiol 14:2741–2756. https://doi.org/10.1111/j.1462-2920.2012.02755.x.
39. Rosso L, Lobry JR, Bajard S, Flandrois JP. 1995. Convenient model to describe the combined effects of temperature and pH on microbial growth. Appl Environ Microbiol 61:610–616.
40. Buescher JM, Liebermeister W, Jules M, Uhr M, Muntel J, Botella E, Hessling B, Kleijn RJ, Le Chat L, Lecointe F, Mader U, Nicolas P, Piersma S, Rugheimer F, Becher D, Bessieres P, Bidnenko E, Denham EL, Dervyn E, Devine KM, Doherty G, Drulhe S, Felicori L, Fogg MJ, Goelzer A, Hansen A, Harwood CR, Hecker M, Hubner S, Hultschig C, Jarmer H, Klipp E, Leduc A, Lewis P, Molina F, Noirot P, Peres S, Pigeonneau N, Pohl S, Rasmussen S, Rinn B, Schaffer M, Schnidder J, Schwikowski B, Van Dijl JM, Veiga P, Walsh S, Wilkinson AJ, Stelling J, Aymerich S, Sauer U. 2012. Global network reorganization during dynamic adaptations of *Bacillus subtilis* metabolism. Science 335:1099–1103. https://doi.org/10.1126/science.1206871.
41. Nicolas P, Mader U, Dervyn E, Rochat T, Leduc A, Pigeonneau N, Bidnenko E, Marchadier E, Hoebeke M, Aymerich S, Becher D, Bisicchia P, Botella E, Delumeau O, Doherty G, Denham EL, Fogg MJ, Fromion V, Goelzer A, Hansen A, Hartig E, Harwood CR, Homuth G, Jarmer H, Jules M, Klipp E, Le Chat L, Lecointe F, Lewis P, Liebermeister W, March A, Mars RAT, Nannapaneni P, Noone D, Pohl S, Rinn B, Rugheimer F, Sappa PK, Samson F, Schaffer M, Schwikowski B, Steil L, Stulke J, Wiegert T, Devine KM, Wilkinson AJ, Maarten van Dijl J, Hecker M, Volker U, Bessieres P, Noirot P. 2012. Condition-dependent transcriptome reveals high-level regulatory architecture in *Bacillus subtilis*. Science 335:1103–1106. https://doi.org/10.1126/science.1206848.
42. Chastanet A, Vitkup D, Yuan G-C, Norman TM, Liu JS, Losick RM. 2010. Broadly heterogeneous activation of the master regulator for sporulation in *Bacillus subtilis*. Proc Natl Acad Sci 107:8486–8491. https://doi.org/10.1073/pnas.1002499107.
43. Veening J-W, Hamoen LW, Kuipers OP. 2005. Phosphatases modulate the bistable sporulation gene expression pattern in *Bacillus subtilis*. Mol Microbiol 56:1481–1494. https://doi.org/10.1111/j.1365-2958.2005.04659.x.
44. Blokpoel MCJ, O'Toole R, Smeulders MJ, Williams HD. 2003. Development and application of unstable GFP variants to kinetic studies of mycobacterial gene expression. J Microbiol Methods 54:203–211. https://doi.org/10.1016/S0167-7012(03)00044-7.
45. Campbell TN, Choy F. 2001. The effect of pH on green fluorescent protein: a brief review. Mol Biol Today 2:1–4.
46. Cormack BP, Valdivia RH, Falkow S. 1996. FACS-optimized mutants of the green fluorescent protein (GFP). Gene 173:33–38. https://doi.org/10.1016/0378-1119(95)00685-0.
47. Guiziou S, Sauveplane V, Chang H-J, Clerté C, Declerck N, Jules M, Bonnet J. 2016. A part toolbox to tune genetic expression in *Bacillus subtilis*. Nucleic Acids Res 44:7495–7508. https://doi.org/10.1093/nar/gkw624.
48. Hageman JH, Shankweiler GW, Wall PR, Franich K, McCowan GW, Cauble SM, Grajeda J, Quinones C. 1984. Single, chemically defined sporulation medium for *Bacillus subtilis*: growth, sporulation, and extracellular protease production. J Bacteriol 160:438–441.
49. Huet S, Bouvier A, Poursat M, Jolivet E. 2003. Statistical tools for nonlinear regression. Springer-Verlag, New York, NY.
50. Abbas AA, Planchon S, Jobin M, Schmitt P. 2014. A new chemically defined medium for the growth and sporulation of *Bacillus cereus* strains in anaerobiosis. J Microbiol Methods 105:54–58. https://doi.org/10.1016/j.mimet.2014.07.006.